AD-A084 857 ARMY MISSILE COMMAND REDSTONE ARSENAL AL TECHNOLOGY LAB F/G 17/9
A MATHEMATICAL ANALYSIS OF POLARIMETRIC PHASE AND AMPLITUDE WIT--ETC(U)
SEP 79 P M ALEXANDER
UNCLASSIFIED DRSMI-T-79-92 NL

1 OF 1
AD
A084857

END
DATE
FILMED
6-80
DTIC

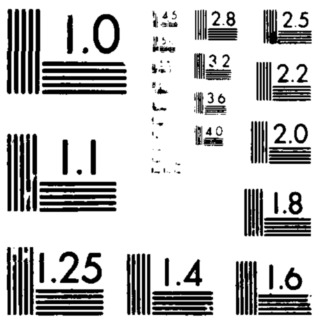

MICROCOPY RESOLUTION TEST CHART
NATIONAL BUREAU OF STANDARDS-1963-A

ADA084857

LEVEL II

1

5C

TECHNICAL REPORT T-79-92

A MATHEMATICAL ANALYSIS OF POLARIMETRIC PHASE AND AMPLITUDE WITH FREQUENCY AGILITY FOR RADAR TARGET ACQUISITION

P. Martin Alexander
Technology Laboratory

24 September 1979

U.S. ARMY MISSILE COMMAND

Redstone Arsenal, Alabama 35809

Approved for public release; distribution unlimited.

SMI FORM 1021, 1 JUL 79 PREVIOUS EDITION IS OBSOLETE

80 5 29 062

DISPOSITION INSTRUCTIONS

DESTROY THIS REPORT WHEN IT IS NO LONGER NEEDED. DO NOT RETURN IT TO THE ORIGINATOR.

DISCLAIMER

THE FINDINGS IN THIS REPORT ARE NOT TO BE CONSTRUED AS AN OFFICIAL DEPARTMENT OF THE ARMY POSITION UNLESS SO DESIGNATED BY OTHER AUTHORIZED DOCUMENTS.

TRADE NAMES

USE OF TRADE NAMES OR MANUFACTURERS IN THIS REPORT DOES NOT CONSTITUTE AN OFFICIAL ENDORSEMENT OR APPROVAL OF THE USE OF SUCH COMMERCIAL HARDWARE OR SOFTWARE.

UNCLASSIFIED

SECURITY CLASSIFICATION OF THIS PAGE (When Data Entered)

REPORT DOCUMENTATION PAGE

READ INSTRUCTIONS BEFORE COMPLETING FORM

1. REPORT NUMBER
T-79-92

2. GOVT ACCESSION NO.
ADA084857

3. RECIPIENT'S CATALOG NUMBER

4. TITLE (and Subtitle)
6
A Mathematical Analysis of Polarimetric Phase and Amplitude with Frequency Agility for Radar Target Acquisition.

5. TYPE OF REPORT & PERIOD COVERED
9
Technical Rep[redacted]t,

6. PERFORMING ORG. RE[redacted]T NUMBER

7. AUTHOR(s)
10
P. Martin Alexander

8. CONTRACT OR GRANT NUMBER(s)

9. PERFORMING ORGANIZATION NAME AND ADDRESS
Commander
US Army Missile Command
ATTN: DRSMI-TEL
Redstone Arsenal, Alabama 35809

10. PROGRAM ELEMENT, PROJECT, TASK AREA & WORK UNIT NUMBERS

11. CONTROLLING OFFICE NAME AND ADDRESS
Commander
US Army Missile Command
ATTN: DRSMI-TI (R&D)
Redstone Arsenal, Alabama 35809

12. REPORT DATE
11
24 Sep[redacted]79

13. NUMBER OF PAGES
40

14. MONITORING AGENCY NAME & ADDRESS (if different from Controlling Office)
12 44

15. SECURITY CLASS. (of this report)
Unclassified

15a. DECLASSIFICATION/DOWNGRADING SCHEDULE

16. DISTRIBUTION STATEMENT (of this Report)

Approved for public release; distribution unlimited.

17. DISTRIBUTION STATEMENT (of the abstract entered in Block 20, if different from Report)

14 DRSMI-T-79-92

18. SUPPLEMENTARY NOTES

19. KEY WORDS (Continue on reverse side if necessary and identify by block number)

LFM Waveform
Polarimetric
Fourier
Trihedral Corner Reflector
Depolarization
Frequency Spectrum
Pseudo-coherent
Elliptical polarization
Monostatic Radar

20. ABSTRACT (Continue on reverse side if necessary and identify by block number)

Target models have been used to generate a mathematical analysis of the output voltage from a frequency agile radar with polarimetric processing. The purpose of the investigation was to determine the usefulness of such a system for target acquisition. It is shown that frequency agility provides a frequency spectrum at the output which is characteristic of the major reflecting centers illuminated by the radar. Polarimetric processing is not required to obtain this information. It is shown that each pair of individual reflectors contributes a frequency to the Fourier transformed signal. For a linearly frequency modulat-

> over

DD FORM 1 JAN 73 1473 EDITION OF 1 NOV 65 IS OBSOLETE

UNCLASSIFIED

SECURITY CLASSIFICATION OF THIS PAGE (When Data Entered)

393427

ed waveform, this frequency depends on the difference in radar range between the two reflectors, the bandwidth of the transmitter, and the repetition period of the LFM waveform.

CONTENTS

ILLUSTRATIONS

1. INTRODUCTION

Recent interest has been shown in using a technique referred to as polarimetric phase processing (or simply, polarimetric processing) for clutter rejection and target discrimination in acquisition and fire control radars [1], [2], [3], [4]. The technique has also been called pseudo-coherent detection (discrimination). A circularly polarized wave is transmitted, and separate horizontal and vertical channels receive the return simultaneously. These two signals are then mixed, using one channel as the local oscillator (hence, "pseudo-coherent"). The resulting signal depends on the relative phase between the horizontal and vertical channels, and this phase difference is called the polarimetric phase.

The underlying assumption of the discrimination technique is that, for any given radar range cell, the resulting polarimetric phase is a function of the transmitted frequency. For example, if a frequency agile radar is linearly frequency modulated (LFM), then the measured signal voltage at the mixer output is a function of time. If this time varying voltage is Fourier analyzed, then the resulting spectrum contains frequencies which are characteristic of the target clutter.

In the present work, target models are used to generate a mathematical analysis of the output signal expected from polarimetric phase processing in an effort to determine the utility of the technique for target acquisition. The general thrust of this effort is toward tactical land combat operations, where discrimination between threat targets (such as tanks) and non-threat targets (jeeps for example) is desired.

In Section 2, a simplistic transmitter receiver system model is described, and the sign convention for a circularly polarized wave is established. In Section 3, the polarization matrix is introduced, and the matrix elements are related to the radar cross section.

Simple targets, consisting of flat plate type reflectors, are described in Section 4, and it is shown that odd bounce reflectors, such as a flat plate or a trihedral corner reflector, reverse the rotational sense of the circularly polarized wave.

A target model, in which the target is assumed to consist of a collection of even bounce and odd bounce type reflectors, is developed in Section 5. An equation is derived which contains the various contributions to the dc signal expected at the mixer output. Some of the terms show a sinusoidal dependence on frequency, while others are frequency independent. It is shown that the interference effect between each pair of individual reflectors contributes a frequency to the Fourier transformed signal. For LFM, this frequency depends only on:

- The difference in radar range between the two reflectors.

- The bandwidth of the frequency agile transmitter.

- The repetition period of the frequency span (the time during which the transmitter spans the bandwidth). Thus, targets can be characterized on the basis of difference in distances between major reflectors.

In the model developed in Section 5, the targets were assumed to cause no depolarization. That is, if circular polarization were transmitted, then any given reflector would return circular polarization. In Section 6, dipole-like targets are considered as reflectors which return elliptical polarization (depolarized returns). It is shown that such reflectors do not contribute frequency independent dc terms to the mixer output. Thus, to the extent that clutter can be characterized as dipoles, the model predicts clutter rejection.

For comparison, an analysis of a system transmitting and receiving linear polarization is developed in Section 7. It is shown that the frequencies obtained in the Fourier transformed signal are the same as those obtained with polarimetric processing.

In Section 8, conclusions drawn from the analyses are given, and the usefulness of polarimetric processing for target acquisition is evaluated.

2. CIRCULAR POLARIZATION

A simplified representation of the transmitter-receiver system used in polarimetric phase processing is shown in *Figure 1*. The output from a frequency agile oscillator is divided and sent to horizontal (H) and vertical (V) channels. The phase of the horizontal channel is delayed by a 90 degree phase shift. It is assumed that the target is in the far-field of the antennas and that the electric fields are plane waves. Using the right-hand coordinate system shown in *Figure 1*, the vertical component of the electric field incident on the target can be written

$$E_x^t = E_o \cos (kz - \omega t) . \tag{1}$$

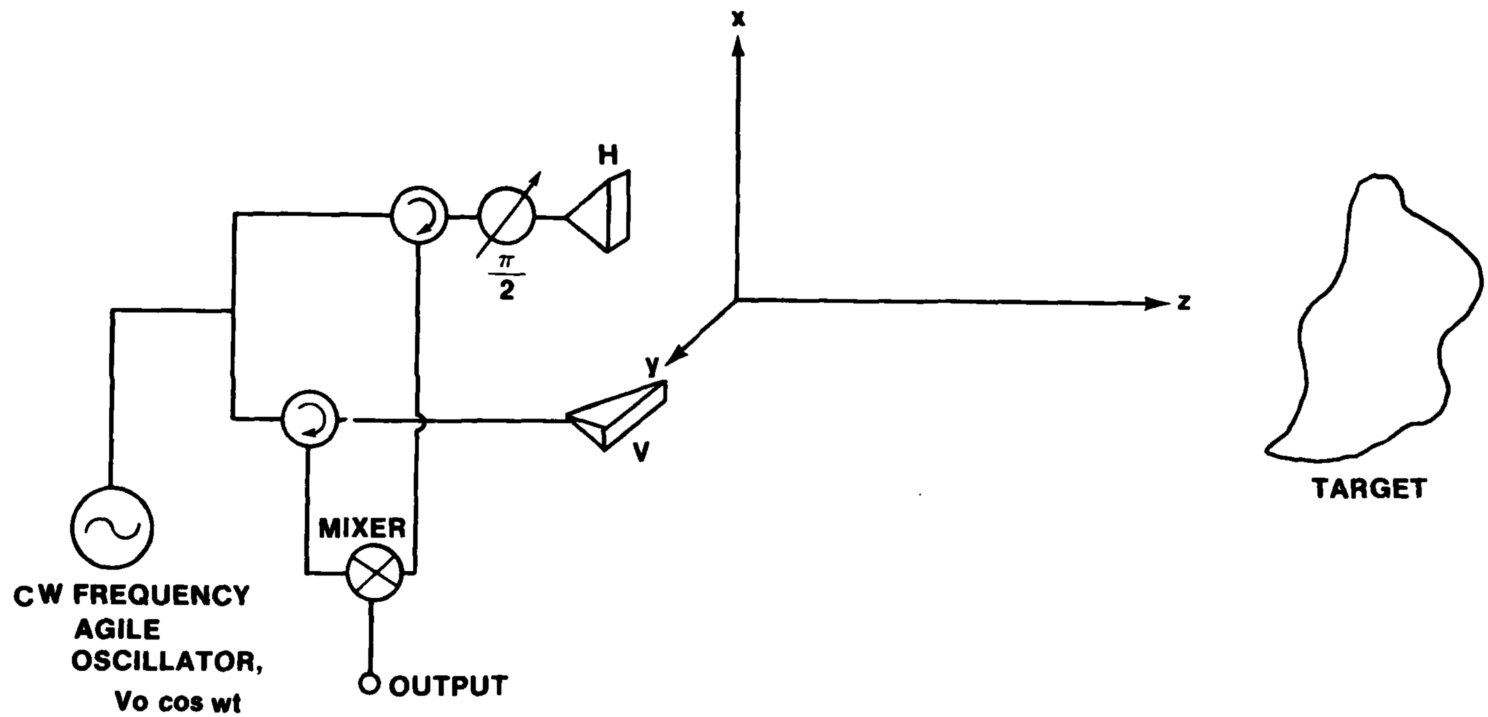

Figure 1. Transmitter-receiver system.

Eo is the electric field amplitude, ω is the carrier angular frequency, and k is the wave number, which depends on the carrier wavelength, λ, according to

$$k = 2\pi/\lambda \quad . \tag{2}$$

The horizonal component is

$$E_y^{\,t} = E_o \cos\,(kz - \omega t - \frac{\pi}{2}) \tag{3}$$

$$= E_o \sin\,(kz - \omega t) \quad . \tag{4}$$

In vector form, the transmitted electric field is

$$E^t = E_o \cos\,(kz - \omega t)\,\vec{x} + E_o \sin\,(k\,z - \omega t)\,\vec{y} \tag{5}$$

where $\vec{x}$ and $\vec{y}$ are unit vectors along the x and y axes, respectively. *Figure 2a* shows the individual components of the electric field, and *Figure 2b* traces the tip of the total rotating electric field vector about the z axis. This polarization, with the wave propagating in the positive z direction, is defined here as right circular polarization (RCP).

For left circular polarization (LCP), the y component of the electric field leads the x component, viz.

$$E_x^{\,t} = E_o \cos\,(kz - \omega t) \tag{6}$$

$$E_y^{\,t} = E_o \cos\,(kz - \omega t + \frac{\pi}{2}) \tag{7}$$

$$= -E_o \sin\,(kz - \omega t) \quad . \tag{8}$$

3. THE POLARIZATION MATRIX

In order to relate the electric field incident on the target to the field returned to the antennas, the polarization matrix is introduced. The "received field", $\vec{E}^r$ is the plane wave impinging on the antennas, assuming that the antennas are in the far-field of the target. If only the vertical component E_x^t is transmitted, the received electric field can be written

$$\vec{E}^{\,r} = a_{xx}\,E_x^{\,t}\,\vec{x} + a_{xy}\,E_x^{\,t}\,\vec{y} \tag{9}$$

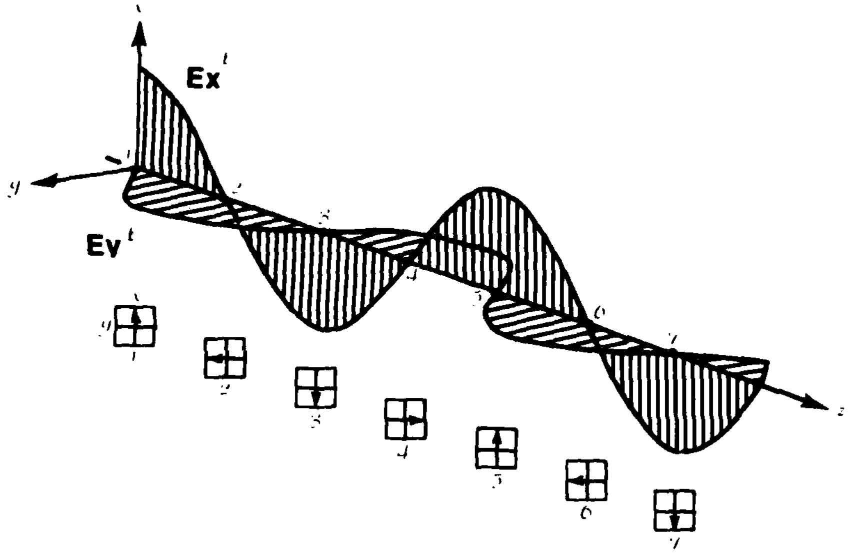

a. Electric field components.

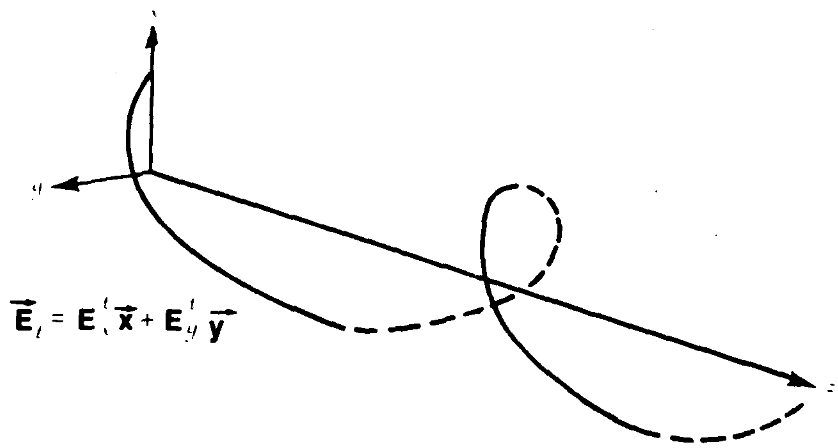

b. Tip of resultant electric field vector.

Figure 2. Right circularly polarized wave (RCP).

where the a's are the electric field coefficients. The a_{xy} coefficient is a measure of *depolarization* since it represents the horizonal reflection obtained from a vertical transmission. A simple example of a depolarizing target is a long thin wire in the x - y plane, but tilted at some angle with respect to the vertical.

Similarly, if only the horizontal component is transmitted, the return can be written

$$\vec{E}^{\,r} = a_{yx}\, E_y^{\,t}\, \vec{x} + a_{yy}\, E_y^{\,t}\, \vec{y}\ . \tag{10}$$

If both components are transmitted, the return is

$$\vec{E}^{\,r} = E_x^{\,r}\, \vec{x} + E_y^{\,r}\, \vec{y} \tag{11}$$

$$= (a_{xx}\, E_x^{\,t} + a_{yx}\, E_y^{\,t})\, \vec{x} + (a_{xy}\, E_x^{\,t} + a_{yy}\, E_y^{\,t})\, \vec{y}\ . \tag{12}$$

In matrix representation, this is

$$\begin{pmatrix} E_x^{\,r} \\ E_y^{\,r} \end{pmatrix} = \begin{pmatrix} a_{xx} & a_{yx} \\ a_{xy} & a_{yy} \end{pmatrix} \begin{pmatrix} E_x^{\,t} \\ E_y^{\,t} \end{pmatrix} \quad , \tag{13}$$

where the two-by-two matrix is called the scattering cross section matrix. It can be shown that, for the case where the receiving antennas and transmitting antennas are at the same location (monostatic radar), the matrix is symmetrical; $a_{yx} = a_{xy}$ [5]. Setting $a_{xx} = a_x$, $a_{yy} = a_y$, and $a_{xy} = a_{yx} = a_d$ (where d implies depolarization), the polarization matrix is

$$\begin{pmatrix} a_x & a_d \\ a_d & a_y \end{pmatrix} . \tag{14}$$

In general, the matrix elements not only contain amplitude information, but also phase information. For example, consider the case of two long thin wires, one horizonal and the other vertical, but separated in range by a distance D. One received component will be shifted in phase with respect to the other by $\omega \frac{2D}{c}$.

It is clear that the electric field coefficients of the polarization matrix (a's) are related to the target radar cross section (RCS). The RCS is defined by

$$\sigma = \lim_{R \to \infty} 4\pi R^2 \frac{|\vec{E}^{\,r}|^2}{|\vec{E}^{\,t}|^2} \tag{15}$$

where:

- R = radar range,
- $\vec{E}^r$ = electric field strength at the receiving antenna, and
- $\vec{E}^t$ = electric field strength incident on the target [6].

The infinite limit on the range R assures that the electric fields impinging on the target and on the receiving antenna are plane waves. If the target is in the far-field of the radar and vice versa, then, to a good approximation, Equation (15) becomes

$$\sigma = 4\pi R^2 \frac{|\vec{E}^{\,r}|^2}{|\vec{E}^{\,t}|^2} \quad . \tag{16}$$

or

$$|\vec{E}^{\,r}| = \frac{\sqrt{\sigma}}{\sqrt{4\pi}\,R} \, |\vec{E}^{\,t}| \quad . \tag{17}$$

Note that there is no phase information in Equation (17).

The above definition of RCS assumes that the receiving antenna can receive whatever polarization that the scattered wave possesses. If one breaks the plane waves into components as before, then an "RCS matrix" similar to the scattering matrix can be defined,

$$\begin{pmatrix} E_x^{\,r} \\ E_y^{\,r} \end{pmatrix} = \frac{1}{\sqrt{4\pi}\,R} \begin{pmatrix} \sqrt{\sigma_{xx}} & \sqrt{\sigma_{yx}} \\ \sqrt{\sigma_{xy}} & \sqrt{\sigma_{yy}} \end{pmatrix} \begin{pmatrix} E_x^{\,t} \\ E_y^{\,t} \end{pmatrix} \quad , \tag{18}$$

where no phase information is retained. Thus, the magnitudes of the scattering matrix elements are given by

$$|a_{ij}| = \frac{\sqrt{\sigma_{ij}}}{\sqrt{4\pi}\,R} \quad . \tag{19}$$

For the monostatic case, the above notation can be simplified as follows:

$$|a_x| = \frac{\sqrt{\sigma_x}}{\sqrt{4\pi}\,R} \quad , \tag{20}$$

$$|a_y| = \frac{\sqrt{\sigma_y}}{\sqrt{4\pi}\,R} \quad , \tag{21}$$

$$|a_d| = \frac{\sqrt{\sigma_d}}{\sqrt{4\pi}\,R} \quad . \tag{22}$$

The electric fields can be expressed in complex notation to facilitate the manipulation of phase shifts. Let transmitted RCP be

$$\vec{E}^{\,t} = \mathrm{Re}\,\{\vec{\mathcal{E}}^{\,t}\} \tag{23}$$

$$= \mathrm{Re}\,\{ e^{j\,(kz\,-\,\omega t)}\,\vec{x} + e^{j\,(kz\,-\,\omega t\,-\,\pi/2)}\,\vec{y}\,\} \quad . \tag{24}$$

where $E_o = 1$ for simplicity. Also for simplicity, the $e^{-j\omega t}$ time dependence will be implied but not expressed, so

$$\vec{\mathcal{E}}^{\,t} = e^{jkz}\,\{\,\vec{x} + e^{-j\pi/2}\,\vec{y}\,\} \quad . \tag{25}$$

Then

$$\begin{pmatrix} \mathcal{E}_x^{\,r} \\ \mathcal{E}_y^{\,r} \end{pmatrix} = \begin{pmatrix} a_x\,e^{-j\theta_x} & a_d\,e^{-j\theta_d} \\ a_d\,e^{-j\theta_d} & a_y\,e^{-j\theta_y} \end{pmatrix} \begin{pmatrix} 1 \\ e^{-j\frac{\pi}{2}} \end{pmatrix} \cdot e^{j2kR} \tag{26}$$

where the a's are now amplitudes only, θ_x, θ_d, θ_y are the corresponding phase shifts, and R is the radar range to some reference point on the target. The phases have been related to that of the transmitted signal at the antennas, so that $z = 2R$.

Equation (26) holds for all targets, no matter how complex. The polarimetric processing involves frequency agility, however, and it is apparent that the a's and θ's of the polarization matrix depend on frequency, and hence on time, in a complicated way. The analysis is simplified if the complex target can be considered as a collection of simple, independent reflectors. Then, the resultant phase shift can be found from superposing the returned electric fields from all reflectors. For the i^{th} reflector in a given range cell,

$$\begin{pmatrix} \mathcal{E}_{x_i}^{\,r} \\ \mathcal{E}_{y_i}^{\,r} \end{pmatrix} = \begin{pmatrix} a_{x_i} & a_{d_i} \\ a_{d_i} & a_{y_i} \end{pmatrix} \begin{pmatrix} 1 \\ e^{-j\frac{\pi}{2}} \end{pmatrix} \cdot e^{j2kR_i} \quad , \tag{27}$$

where R_i is the range to the i^{th} reflector.

For a given range cell with n reflectors,

$$\mathcal{E}_x^{\,r} = \sum_{i=1}^{n} \mathcal{E}_{x_i}^{\,r} \quad , \tag{28}$$

$$\mathcal{E}_y^{\,r} = \sum_{i=1}^{n} \mathcal{E}_{y_i}^{\,r} \quad . \tag{29}$$

4. SIMPLE REFLECTORS

Consider now the polarization matrix for a few simple reflectors, beginning with a flat metal plate perpendicular to the incident RCP wave (see *Figure 3a*). The vertical component is reflected totally vertical (i.e., there is no depolarization) but with a phase shift of 180 degrees at the plate surface. This phase shift is the result of the requirement that the electric field inside a perfect conductor is always zero. The horizontal component also experiences a 180 degree phase shift, and one would be led to believe that there is no net phase change between vertical and horizontal components. This is not the case, however, because the propagational direction has changed. In order to understand the phases seen by the antennas, consider the primed coordinate system in *Figure 3b*. With respect to this "antenna" coordinate system, it is easy to see that the reflected wave is LCP. The net effect of the reflection, from the viewpoint of the antennas, is that one component has been shifted in phase by 180 degrees relative to the other component. RCP will be changed to LCP, and vice versa. So, the phases of the polarization matrix can be written

$$\begin{pmatrix} -1 & 0 \\ 0 & 1 \end{pmatrix} \quad . \tag{30}$$

Now, in prelude to analyzing returns from multiple bounce reflectors, consider reflection from an infinite plate at an angle with respect to the plane of the incident wave (see *Figure 4*). The vertical component of the transmitted wave is reflected as before with a 180 degree phase shift. The horizontal component is broken down into two further components:

- A component perpendicular to the plate, which experiences no phase shift
- A component parallel to the plate, which is shifted by 180 degrees

As can be seen from *Figure 4*, the reflected wave is still the opposite polarization from that transmitted.

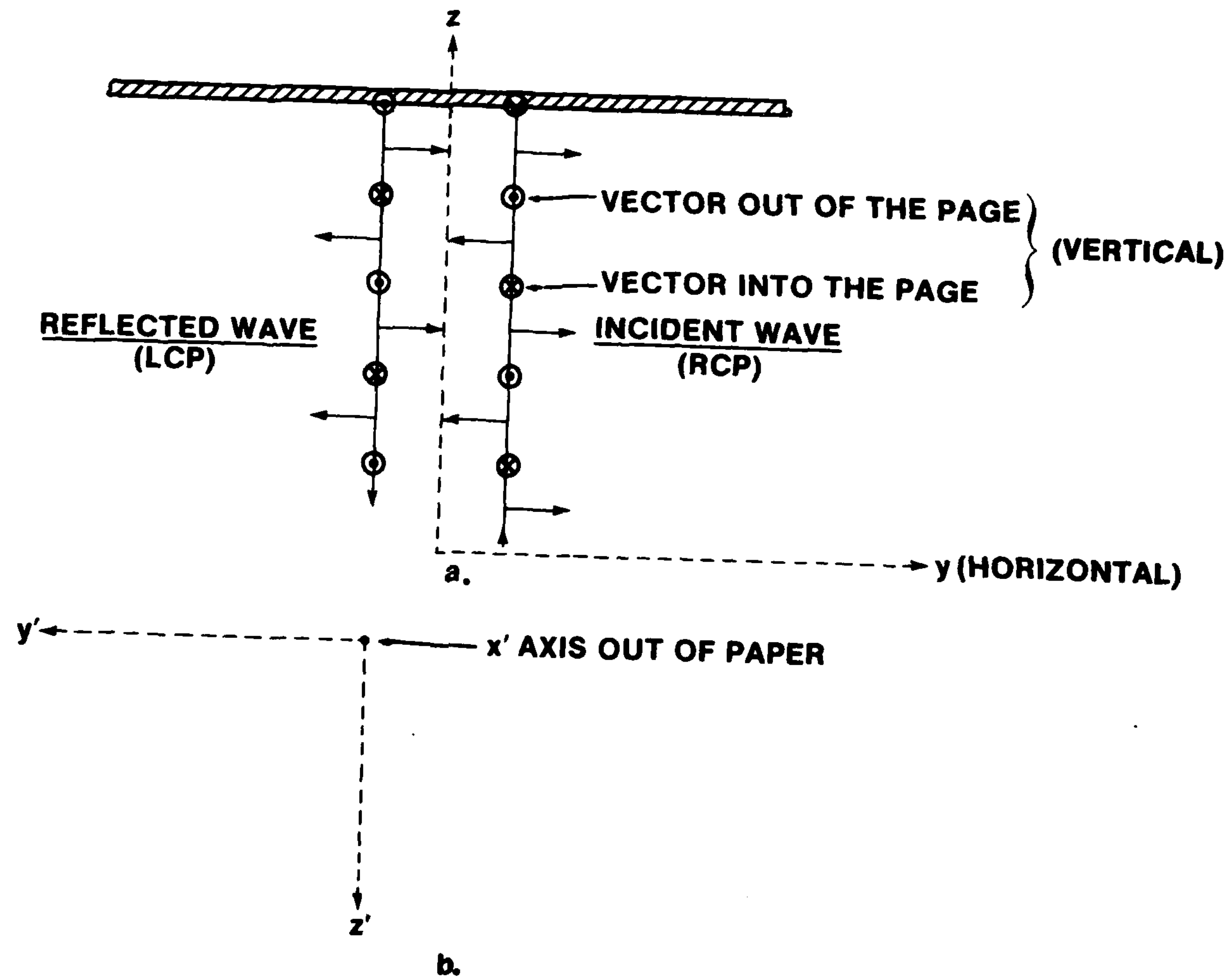

Figure 3. RCP incident on flat plate.

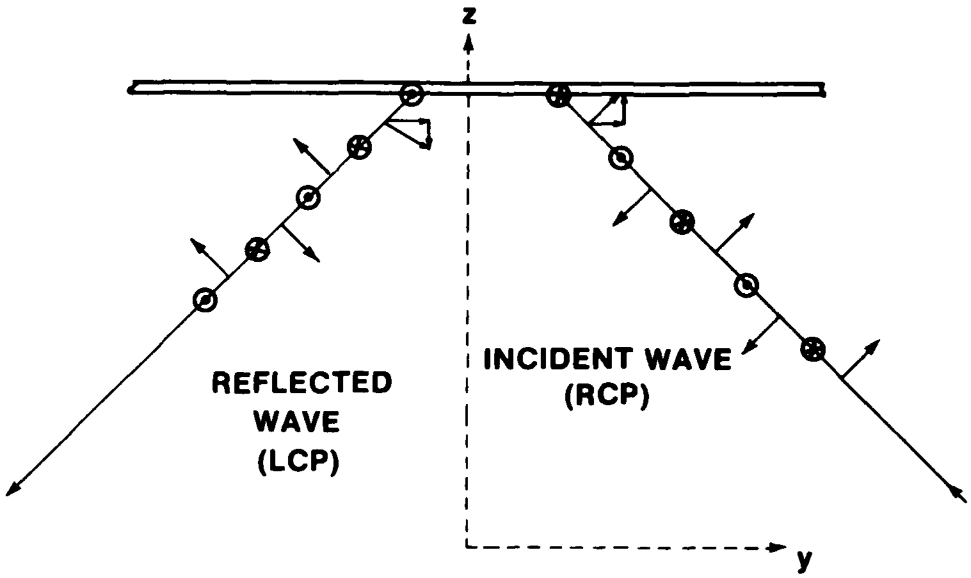

Figure 4. RCP incident at angle with respect to flat plate.

The above result shows that at every bounce from a surface, the sense of the polarization is changed. For a dihedral corner reflector, the wave is returned in its original polarization. In general, an odd bounce target changes the polarization sense; an even bounce target does not. The polarization matrices (phases only) are:

$$\begin{pmatrix} -1 & 0 \\ 0 & 1 \end{pmatrix} \text{ for odd bounce targets,} \tag{31}$$

$$\begin{pmatrix} 1 & 0 \\ 0 & 1 \end{pmatrix} \text{ for even bounce targets.} \tag{32}$$

5. TARGET MODEL

For a target model consisting of flat plates only (dihedral, trihedral corners, etc.), from Equations (19), (26), (28), and (29), the reflected wave is given by

$$\mathscr{E}_x^{\,r} = \sum_{\substack{i=1 \\ \text{odd} \\ \text{bounce} \\ \text{reflectors}}}^{n} \frac{\sqrt{\sigma_{xi}}}{\sqrt{4\pi}\; R_i} (-1)\, e^{j2kR_i}$$

$$+ \sum_{\substack{\ell=1 \\ \text{even} \\ \text{bounce} \\ \text{reflectors}}}^{m} \frac{\sqrt{\sigma_{x\ell}}}{\sqrt{4\pi}\; R_\ell}\, e^{j2kR_\ell} , \tag{33}$$

$$\mathscr{E}_y^{\,r} = \sum_{\substack{i=1 \\ \text{odd} \\ \text{bounce} \\ \text{reflectors}}}^{n} \frac{\sqrt{\sigma_{yi}}}{\sqrt{4\pi}\; R_i}\, e^{-j\frac{\pi}{2}}\, e^{j2kR_i}$$

$$+ \sum_{\substack{\ell=1 \\ \text{even} \\ \text{bounce} \\ \text{reflectors}}}^{m} \frac{\sqrt{\sigma_{y\ell}}}{\sqrt{4\pi}\; R_\ell}\, e^{-j\frac{\pi}{2}}\, e^{j2kR_\ell} . \tag{34}$$

The -1 in the first term of equation (33) is the only effect of phase shifts due to reflection. In Equations (33) and (34) above, the subscript "i" is used to denote odd bounce reflectors only, while the subscript "ℓ" indicates even bounce reflectors. The RCS matrix elements, σ, now have two subscripts, the first indicating x or y direction, and the second indicating the particular reflector.

The voltages at the mixer must now be related to the electric fields at the antennas. Referring to *Figure 1*, the terminal voltages at the antennas are related to the electric field vector at the antennas by

$$V = \vec{h} \cdot \vec{E}^{\,r} . \tag{35}$$

The vector $\vec{h}$ is defined as the effective height of a given antenna, i.e., the effective distance along the antenna over which the field acts. The complex voltages for identical ideal horizontal and vertical horns are

$$V_V = h\, \mathcal{E}_x^r \quad , \tag{36}$$

$$V_H = h\, \mathcal{E}_y^r \quad . \tag{37}$$

The horizontal component is delayed by 90 degrees, so at the mixer,

$$V_H = h\, \mathcal{E}_y^r\, e^{-j\frac{\pi}{2}} \quad . \tag{38}$$

The output of the mixer is proportional to the product of the two voltages (neglecting attenuation losses):

$$V_m = V_V\, V_H \quad , \tag{39}$$

where the constant of proportionality has been set to 1. Using Equations (33), (34), and (38), Equation (39) becomes

$$V_m = \frac{h^2}{4\pi}\left[\sum_{\substack{i=1\\ \text{odd}}}^{n} \frac{\sqrt{\sigma_{xi}}}{R_i}\,(-1)\, e^{j2kR_i} + \sum_{\substack{\ell=1\\ \text{even}}}^{m} \frac{\sqrt{\sigma_{x\ell}}}{R_\ell}\, e^{j2kR_\ell}\right] .$$

$$\left[\sum_{\substack{i=1\\ odd}}^{n} \frac{\sqrt{\sigma_{yi}}}{R_i}\, e^{-j\pi}\, e^{j2kR_i} + \sum_{\substack{\ell=1\\ even}}^{m} \frac{\sqrt{\sigma_{y\ell}}}{R_\ell}\, e^{-j\pi}\, e^{j2kR_\ell}\right] \tag{40}$$

$$= -\frac{h^2}{4\pi}\left[\sum_{\substack{i=1\\ odd}}^{n} \frac{\sqrt{\sigma_{xi}}}{R_i}\, e^{j2kR_i} - \sum_{\substack{\ell=1\\ even}}^{m} \frac{\sqrt{\sigma_{x\ell}}}{R_\ell}\, e^{j2kR_\ell}\right] \cdot$$

$$\left[\sum_{\substack{i=1\\ odd}}^{n} \frac{\sqrt{\sigma_{yi}}}{R_i}\, e^{j2kR_i} + \sum_{\substack{\ell=1\\ even}}^{m} \frac{\sqrt{\sigma_{y\ell}}}{R_\ell}\, e^{j2kR_\ell}\right] , \tag{41}$$

where in Equation (41) $e^{-j\pi}$ has been set equal to -1.

Consider now the two simple cases of a single odd bounce target and a single even bounce target. For an odd bounce target,

$$V_m = -\frac{h^2}{4\pi}\frac{\sqrt{\sigma_x \sigma_y}}{R^2} \cos^2 (2kR - \omega t) \quad , \tag{42}$$

and for an even bounce target

$$V_m = \frac{h^2}{4\pi}\frac{\sqrt{\sigma_x \sigma_y}}{R^2} \cos^2 (2\ kR - \omega t) \quad , \tag{43}$$

where the voltages are now real, and the time dependence is given explicitly. Since

$$\cos^2 (2\ kR - \omega t) = \tfrac{1}{2} + \tfrac{1}{2} \cos \left[2(2kR - \omega t)\right] \quad , \tag{44}$$

the dc voltage component at the mixer output is

$$V_{dc} = \begin{cases} -\dfrac{h^2}{8\pi}\dfrac{\sqrt{\sigma_x\sigma_y}}{R^2} & \text{for single odd bounce target} \quad (45) \\ \dfrac{h^2}{8\pi}\dfrac{\sqrt{\sigma_x\sigma_y}}{R^2} & \text{for single even bounce target.} \quad (46) \end{cases}$$

For a complex target consisting of a collection of m even and n odd bounce reflectors (using "i" and "p" for odd bounce reflector subscripts and "ℓ" and "q" to denote even bounce reflectors) Equation (41) becomes

$$V_m = -\frac{h^2}{4\pi}\Bigg[\sum_{\substack{i=1\\ \text{odd}}}^{n}\sum_{\substack{p=1\\ \text{odd}}}^{n}\frac{\sqrt{\sigma_{xi}\sigma_{yp}}}{R_i\,R_p}\cos(2kR_i - \omega t)\cos(2kR_p - \omega t) + \sum_{\substack{i=1\\ \text{odd}}}^{n}\sum_{\substack{\ell=1\\ \text{even}}}^{m}\frac{\sqrt{\sigma_{xi}\sigma_{y\ell}}}{R_i\,R_\ell}\cos(2kR_i$$

$$- \omega t)\cos(2kR_\ell - \omega t) - \sum_{\substack{i=1\\ \text{odd}}}^{n}\sum_{\substack{\ell=1\\ \text{even}}}^{m}\frac{\sqrt{\sigma_{x\ell}\sigma_{yi}}}{R_i\,R_\ell}\cos(2kR_i$$

$$- \omega t)\cos(2kR_\ell - \omega t) - \sum_{\substack{\ell=1\\ \text{even}}}^{m}\sum_{\substack{q=1\\ \text{even}}}^{m}\frac{\sqrt{\sigma_{y\ell}\sigma_{xq}}}{R_\ell\,R_q}\cos(2kR_\ell$$

$$- \omega t)\cos(2kR_q - \omega t)\Bigg] \,. \quad (47)$$

Using the formula

$\cos A \cos B = {}^1/_2 \cos(A - B) + {}^1/_2 (A + B)$,

keeping only the dc terms, and combining the two middle terms gives

$$V_{dc} = -\frac{h^2}{8\pi}\left[\sum_{\substack{i=1\\ odd}}^{n} \frac{\sqrt{\sigma_{xi}\sigma_{yi}}}{R_i^{\,2}} + \sum_{\substack{i=1\\ odd\\ i\neq p}}^{n} \sum_{\substack{p=1\\ odd}}^{n} \frac{\sqrt{\sigma_{xi}\sigma_{yp}}}{R_i\,R_p} \cos\left[2k(R_i - R_p)\right] + \sum_{\substack{i=1\\ odd}}^{n} \sum_{\substack{\ell=1\\ even}}^{m} \frac{\sqrt{\sigma_{xi}\sigma_{y\ell}} - \sqrt{\sigma_{yi}\sigma_{x\ell}}}{R_i\,R_\ell} \cos\left[2k(R_i - R_\ell)\right] - \sum_{\substack{\ell=1\\ even}}^{m} \frac{\sqrt{\sigma_{x\ell}\sigma_{y\ell}}}{R_\ell^{\,2}} - \sum_{\substack{\ell=1\\ even\\ \ell\neq q}}^{m} \sum_{\substack{q=1\\ even}}^{m} \frac{\sqrt{\sigma_{y\ell}\sigma_{xq}}}{R_\ell\,R_q} \cos\left[2k(R_\ell - R_q)\right]\right] . \tag{48}$$

Upon examining Equation (48) term by term, one finds two terms with no cosine factors:

$$-\frac{h^2}{8\pi} \sum_{\substack{i=1\\ odd}}^{n} \frac{\sqrt{\sigma_{xi}\sigma_{yi}}}{R_i^{\,2}} \quad \text{and} \quad \frac{h^2}{8\pi} \sum_{\substack{\ell=1\\ even}}^{m} \frac{\sqrt{\sigma_{x\ell}\sigma_{y\ell}}}{R_\ell^{\,2}} .$$

These terms represent the "self-interference" effects for each individual reflector in the complex target. These terms are the same as found in Equations (45) and (46) for single reflectors. The term

$$-\frac{h^2}{8\pi} \sum_{\substack{i=1\\ odd\\ i\neq p}}^{n} \sum_{\substack{p=1\\ odd}}^{n} \frac{\sqrt{\sigma_{xi}\sigma_{yp}}}{R_i R_p} \cos\left[2k(R_i - R_p)\right]$$

represents the odd bounce reflectors interfering with each other. For the case of only two odd bounce reflectors, this term becomes

$$- \frac{h^2}{8\pi} \frac{\sqrt{\sigma_{x_1}\sigma_{y_2}} + \sqrt{\sigma_{x_2}\sigma_{y_1}}}{R_1 R_2} \cos \left[2k(R_1 - R_2)\right] .$$

Similarly, the term

$$\frac{h^2}{8\pi} \sum_{\substack{\ell=1 \\ \text{even}}}^{m} \sum_{\substack{q=1 \\ \text{even} \\ \ell \neq q}}^{m} \frac{\sqrt{\sigma_{y\ell}\sigma_{xq}}}{R_\ell R_q} \cos \left[2k(R_\ell - R_q)\right]$$

represents the interference effects between even bounce reflectors.

The remaining term,

$$- \frac{h^2}{8\pi} \sum_{\substack{i=1 \\ \text{odd}}}^{n} \sum_{\substack{\ell=1 \\ \text{even}}}^{m} \frac{\sqrt{\sigma_{xi}\sigma_{y\ell}} - \sqrt{\sigma_{yi}\sigma_{x\ell}}}{R_i R_\ell} \cos \left[2k(R_i - R_\ell) ,\right]$$

represents the interference between each even bounce reflector and each odd bounce reflector. Note that if each reflector is symmetric with respect to RCS, i.e., if $\sigma_x = \sigma_y$ for all reflectors, then this term is zero.

Recall that the wave number k is related to the angular frequency of the radar ω by $\omega = k c$, where c is the propagation velocity. From the above terms it is clear that, if the frequency is varied or stepped as a function of time, the "dc" signal also varies as a function of time. This time variation, however, is not only due to the fact that the cosine arguments are a function of time, but also is due to the dependence of RCS on wavelength. For the flat plate type targets (including corner reflectors) assumed in this analysis, the RCS for normal incidence is given by

$$\sigma_x = \sigma_y = \frac{4\pi A^2}{\lambda^2} , \tag{49}$$

where A is the area of the aperture [7]. Using Equation (48) for two odd bounce scatterers with aperture areas A_1 and A_2 gives

$$V_{dc} = -\frac{h^2}{2\lambda^2}\left[\frac{A_1^{\,2}}{R_1^{\,2}} + \frac{A_2^{\,2}}{R_2^{\,2}} + \frac{2\,A_1\,A_2}{R_1\,R_2}\cos\left[2k(R_1 - R_2)\right]\right] \quad . \tag{50}$$

Assume now that the frequency increases linearly with time, (see *Figure 5*), so that

$$f = f_o + \frac{f_B}{T}\,t \quad , \quad t < T \; , \tag{51}$$

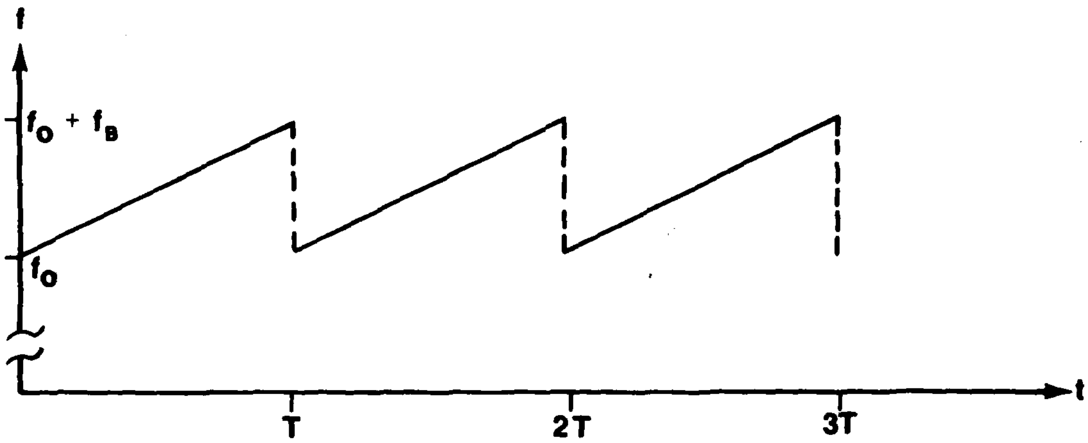

Figure 5. Linear frequency modulation.

where:

- f_o = starting frequency,
- f_B = bandwidth of frequency agile transmitter, and
- T = repetition period of frequency span.

Note that a linearly stepped frequency is equivalent, as long as the signal is sampled once for each step. The $1/\lambda^2$ gives a nonlinear decrease of the overall signal level during T. For $f_o = 35$ GHz and $f_B = 500$ MHz, this variation amounts to 2.8 percent. The information of interest, i.e., the frequency spectra characteristic of the target, is contained in

$$V_f = \cos\left[2k(R_1 - R_2)\right] \quad . \tag{52}$$

Using $k = \frac{\omega}{c} = 2\pi\, f/c$ gives

$$V_f = \cos\left[\frac{4\pi\ (R_1 - R_2)}{c}\left(f_o + \frac{f_B t}{T}\right),\right] \tag{53}$$

which can be written

$$V_f = \cos\ (2\pi\ f_{12}\ t + \phi) \tag{54}$$

where ϕ is a constant phase angle.

$$\phi = \frac{4\pi\ (R_1 - R_2)}{c}\ f_o \quad , \tag{55}$$

and f_{12} is the target characteristic frequency given by

$$\boxed{f_{12} = \frac{2\ |\ R_1 - R_2\ |\ f_B}{c\ T}\ .} \tag{56}$$

Note that this frequency is independent of the starting frequency fo. If, for example, $|R_1 - R_2| =$ 1 m, $f_B = 500$ MHz, and $T = 3$ ms, then $f_{12} = 1$ KHz.

From Equation (56), it is clear that the frequency spectrum of the received signal for a complex target contains frequencies given by

$$f_{ij} = \frac{2\ |\ R_i - R_j\ |\ f_B}{c\ T} \quad , \tag{57}$$

so that a given target can be characterized by the difference in range

$$d_{ij} = |\ R_i - R_j\ | \tag{58}$$

between individual reflectors. For example, a man-made target (vehicle) might consist of two major reflectors separated in range by ~ 1 m. The clutter might consist of a large number of randomly distributed reflectors whose d_{ij}, and hence f_{ij}, could be described by a gaussian probability density,

$$p\,(f_{ij}) = \frac{1}{\sqrt{2\pi}\;\sigma}\; e^{-\frac{1}{2}\left(\frac{f_{ij} - \mu}{\sigma}\right)^2} \tag{59}$$

where μ is the mean frequency and σ is the standard deviation of the distribution. Suppose the clutter can be characterized as reflectors separated by a mean distance of 2m with a standard deviation of 0.25m. Using the same numbers as before for the target (d_{12} = 1 m) and the radar (f_B = 500 MHz, T = 3ms), then the frequency spectrum will resemble *Figure 6*. The target can be distinguished from the clutter if the difference between the target characteristic frequency and the mean clutter frequency is large compared to the clutter frequency spread.

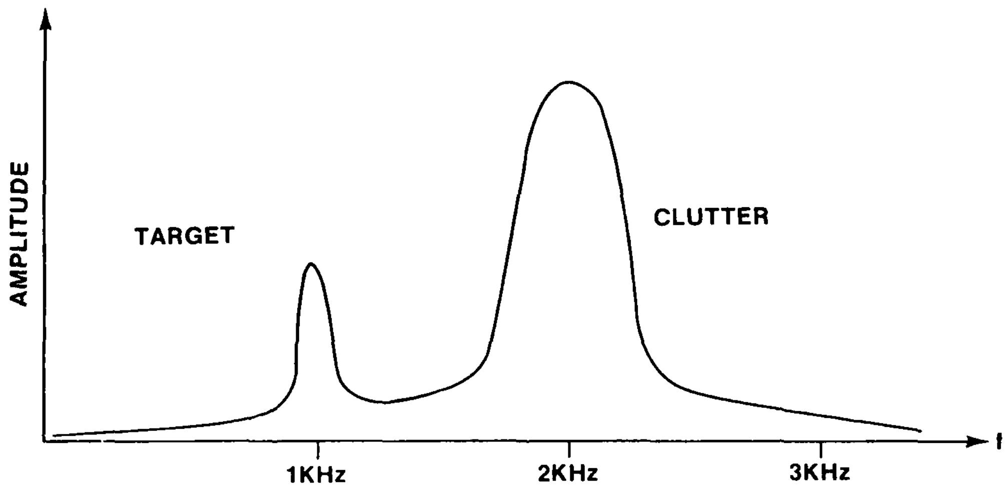

Figure 6. Frequency spectrum for target/clutter model.

Similarly, if two different targets have sufficiently different reflector range characteristics, then target classification, based on measured data at various target aspect angles, may be possible.

6. DEPOLARIZING TARGETS

Up to now, no targets which depolarize have been considered; metal edges and thin wires (dipoles) are targets giving depolarized returns. If the radius of curvature of the wire (or edge) is small compared to the transmitted wavelength, then the RCS for normal incidence and electric field vector parallel to the wire is

$$\sigma \simeq \frac{L^2}{\pi} \tag{60}$$

where L is the length of the wire [5]. If the wire is at an angle θ relative to the vertical, the polarization matrix is given by

$$\begin{pmatrix} \mathcal{E}_{xi}^{r} \\ \mathcal{E}_{yi}^{r} \end{pmatrix} = \frac{L_i}{2\pi R_i} \begin{pmatrix} -\cos^2\theta_i & -\cos\theta_i \sin\theta_i \\ \cos\theta_i \sin\theta_i & \sin^2\theta_i \end{pmatrix} \begin{pmatrix} E_x^{t} \\ E_y^{t} \end{pmatrix} \tag{61}$$

for an odd bounce reflector; the minus signs go out for an even bounce reflector. It is expected that, since the RCS of a wire is much less than that of a plate, the returns from multiple bounces between wires, and between wires and plates, can be neglected.

For a collection of n wires,

$$\begin{aligned} \mathcal{E}_x^{r} = &- \sum_{i=1}^{n} \frac{L_i}{2\pi R_i} \cos^2\theta_i \, e^{j2kR_i} \\ &- \sum_{i=1}^{n} \frac{L_i}{2\pi R_i} \cos\theta_i \sin\theta_i \, e^{-j\frac{\pi}{2}} e^{j2kR_i} \; ; \end{aligned} \tag{62}$$

$$\begin{aligned} \mathcal{E}_y^{r} = &\sum_{i=1}^{n} \frac{L_i}{2\pi R_i} \cos\theta_i \sin\theta_i \, e^{j2kR_i} \\ &+ \sum_{i=1}^{n} \frac{L_i}{2\pi R_i} \sin^2\theta_i \, e^{-j\frac{\pi}{2}} e^{j2kR_i} \; . \end{aligned} \tag{63}$$

The voltage appearing at the output of the mixer is

$$
\begin{aligned}
V_m = \frac{h^2}{4\pi^2} & \left[\sum_{i=1}^{n} \frac{L_i}{R_i} e^{2kR_i} \left(\cos^2 \theta_i \right.\right. \\
& \left.\left. + \cos \theta_i \sin \theta_i e^{-j\pi/2} \right) \right] \qquad (64)
\end{aligned}
$$

$$
\left[\sum_{i=1}^{n} \frac{L_i}{R_i} e^{2kR_i} \left(\sin^2 \theta_i - \cos \theta_i \sin \theta_i e^{-j\pi/2} \right) \right]
$$

$$
\begin{aligned}
= \frac{h^2}{4\pi^2} & \left[\sum_{i=1}^{n} \frac{L_i^2}{R_i^2} \cos^2 \theta_i \sin^2 \theta_i \cos^2 (2kR_i - \omega t) \right. \\
& + \sum_{\substack{i=1 \\ i \neq j}}^{n} \sum_{j=1}^{n} \frac{L_i L_j}{R_i R_j} \cos^2 \theta_i \sin^2 \theta_j \cos(2kR_i \\
& - \omega t) \cos(2kR_j - \omega t) - \sum_{i=1}^{n} \frac{L_i^2}{R_i^2} \cos^3 \theta_i \sin \theta_i \\
& \cos(2kR_i - \omega t) \sin(2kR_i - \omega t) - \sum_{\substack{i=1 \\ i \neq j}}^{n} \sum_{j=1}^{n} \frac{L_i L_j}{R_i R_j} \\
& \cos^2 \theta_i \cos \theta_j \sin \theta_j \cos(2kR_i - \omega t) \sin(2kR_j - \omega t) \\
& + \sum_{i=1}^{n} \frac{L_i^2}{R_i^2} \cos \theta_i \sin^3 \theta_i \sin(2kR_i - \omega t) \cos(2kR_i - \omega t)
\end{aligned}
$$

$$+ \sum_{\substack{i=1 \\ i \neq j}}^{n} \sum_{j=1}^{n} \frac{L_i L_j}{R_i R_j} \cos \theta_i \sin \theta_i \sin^2 \theta_j \sin(2kR_i - \omega t)$$

$$\cos(2kR_j - \omega t) - \sum_{i=1}^{n} \frac{L_i^2}{R_i^2} \cos^2 \theta_i \sin^2 \theta_i \sin^2(2kR_i - \omega t)$$

$$- \sum_{\substack{i=1 \\ i \neq j}}^{n} \sum_{j=1}^{n} \frac{L_i L_j}{R_i R_j} \cos \theta_i \sin \theta_i \cos \theta_j \sin \theta_j \sin(2kR_i - \omega t)$$

$$\left. \sin(2kR_j - \omega t) \right] . \tag{65}$$

Using trigonometric identities and keeping only the dc terms gives

$$V_{dc} = \frac{h^2}{8\pi} \sum_{\substack{i=1 \\ i \neq j}}^{n} \sum_{j=1}^{n} \frac{L_i L_j}{R_i R_j} \left[\cos^2 \theta_i \sin^2 \theta_j \cos 2k(R_i - R_j) \right.$$

$$+ \cos^2 \theta_i \cos \theta_j \sin \theta_j \sin 2k(R_i - R_j)$$

$$+ \cos \theta_i \sin \theta_i \sin^2 \theta_j \sin 2k(R_i - R_j)$$

$$\left. - \cos \theta_i \sin \theta_i \cos \theta_j \sin \theta_j \cos 2k(R_i - R_j) \right] , \tag{66}$$

or

$$\boxed{V_{dc} = \frac{h^2}{8\pi} \sum_{\substack{i=1 \\ i \neq j}}^{n} \sum_{j=1}^{n} \frac{L_i L_j}{R_i R_j} \left[A_{ij} \cos 2k(R_i - R_j) + B_{ij} \sin 2k(R_i - R_j) \right]} \tag{67}$$

where

$$A_{ij} \equiv \cos^2 \theta_i \sin^2 \theta_j - \cos \theta_i \sin \theta_i \cos \theta_j \sin \theta_j \ ; \quad (68)$$

$$B_{ij} \equiv \cos^2 \theta_i \cos \theta_j \sin \theta_j + \sin \theta_i \cos \theta_i \sin^2 \theta_j \ . \quad (69)$$

Notice that all of the "self interference" terms have gone out of the mixer dc output; a single wire target gives no signal in polarimetric processing. If clutter can be characterized as being more like wires (trees, long grass, etc.) and targets characterized more by flat plates and corner reflectors, then the polarimetric processing technique should provide clutter rejection for the general dc signal at any given frequency.

For the simple case of two wires, one horizontal and one vertical, the signal is

$$V_{dc} = \frac{h^2}{8\pi} \frac{L_1 L_2}{R_1 R_2} \cos 2k(R_i - R_j) \quad , \qquad (70)$$

as one might intuitively expect. For the case of a collection of wire like reflectors which are all oriented at the same angle, θ,

$$V_{dc} = \frac{h^2}{4\pi} \sin 2\theta \sum_{i=1}^{n} \sum_{\substack{j=1 \\ i \neq j}}^{n} \frac{L_i L_j}{R_i R_j} \sin 2k(R_i - R_j) \ . \qquad (71)$$

Thus, for $\theta = 0$ degrees or 90 degrees, there is no return. One can expect that for trees, weeds, and tall grass which are approximately vertical, the frequency dependent dc terms are zero, and this results in clutter rejection in frequency space. To the extent that clutter can be characterized by randomly-oriented, dipole-like reflectors which depolarize, one can expect some clutter rejection using polarimetric processing.

For an extension to the more general case of a target consisting of both wire-like and plate-like reflectors, only the additional cross terms between Equations (62), (63) and (33), (34) remain to be considered. It is obvious that the interference between each wire and each plate target contributes a frequency to the spectrum.

7. LINEARLY POLARIZED RADAR

For comparison, an analysis of a system transmitting and receiving linear polarization is developed. For vertical transmit and receive, the electric field is given by

$$\mathscr{E}_x^r = - \sum_{\substack{i=1 \\ \text{odd bounce} \\ \text{reflectors}}}^{n_1} \frac{\sqrt{\sigma_{xi}}}{\sqrt{4\pi}\, R_i} e^{j2kR_i} + \sum_{\substack{\ell=1 \\ \text{even} \\ \text{bounce} \\ \text{reflectors}}}^{n_2} \frac{\sqrt{\sigma_{x\ell}}}{\sqrt{4\pi}\, R_\ell} e^{j2kR_\ell}$$

$$+ \sum_{\substack{m=1 \\ \text{wire-type} \\ \text{reflectors}}}^{n_3} \frac{L_m}{2\pi R_m} \sin^2 \theta_m \, e^{2kR_m} \quad . \tag{72}$$

The output signal is found from squaring the voltage signal at the antenna.

$$V_m = h^2 \, (\mathscr{E}_x^r)^2 \, . \tag{73}$$

Using the trigonometric identities, and keeping only dc terms as before, gives similar results as for polarimetric processing. There is a frequency in the spectrum resulting from the interference between each pair of reflectors, but there are now dc terms independent of frequency resulting from the "self-interference" effects of the wire-like reflectors. For a linearly frequency modulated signal, the frequency spectra of the returned signal will contain the

$$f_{ij} = \frac{2 \mid R_i - R_j \mid f_B}{c \; T} \tag{57}$$

as before, but the amplitudes now depend only on the σ_{xx} element of the RCS matrix. It should be pointed out that the same "clutter rejection" obtained for vertical trees, grass, etc. with polarimetric processing can be achieved here by transmitting a horizontal linearly polarized wave.

8. CONCLUSIONS

For the flat plate/corner reflector target model assumed, Equation (48) shows that the resulting signal can be a bipolar response as a function of frequency. Intuitively, one might expect that a bipolar signal results from a complex target, because such a target is a collection of even bounce and odd bounce scatterers which result in a combination of those terms given in Equations (45) and (46). Equation (48) shows however, that these terms are frequency independent. In fact, the minimum condition for achieving a bipolar response requires that the target contain two even bounce scatterers and two odd bounce scatterers. Not only must these four scatterers be present, but they also must be appropriately spaced in range, i.e., the two odd bounce targets must be constructively interferring while the two even bounce targets are destructively interferring, and vice versa. This seems a rather broad assumption on which one presumes to be able to discriminate between a tank (complex target) and a decoy (single corner reflector).

It was shown, however, that polarimetric processing does in fact provide a method of obtaining a characteristic target spectrum (Fourier transform of the mixer signal) using frequency agility. The characteristic frequencies depend on the range difference between target reflectors, on the LFM bandwidth, and on the FM repetition rate (Equation (57)). If targets and clutter have sufficiently unique range distributions for individual reflectors (for example, a characteristic average inter-reflector distance), then clutter rejection and target classification in frequency space may be possible.

It was also shown that, for clutter which can be characterized as depolarizing dipoles, a reduction of the overall dc signal due to clutter results. There is evidence which does in fact indicate that clutter depolarizes more than hard targets. It has been shown that, at microwave frequencies, σ_{xx}/σ_{xy} is ~ 4 dB for distributed clutter (trees) and 8 - 10 dB for vehicles [3]. This clutter rejection occurs, however, in the dc terms which are frequency independent. If the desired target/clutter discriminants are the frequency spectra due to frequency agility, it is not clear to what extent this "clutter rejection" enhances the signal to noise ratio in the frequency domain.

Finally, it was shown that target/clutter discrimination based on the Fourier transform of the received signal is not indigenous to polarimetric processing; the technique can be realized using linearly polarized radar. In short, there are two entirely separate effects involved in the system model:

- Polarimetric processing which results in rejection of dipole-like clutter.

- Frequency agility which creates the possibility of characterizing targets in frequency space due to interference effects.

REFERENCES

1. Reedy, E. K., Eaves, J. L., Piper, S. O., Parks, W. K., Brookshire, S. P., Wetherington, R. D., and Trebits, R. N., (C) *Stationary Target Detection and Classification Studies (U), 2nd Interim Report*, US Army Electronics Research and Development Command, No. ECOM-76-0961-2, March 1978.

2. Root, Jr. L. W. (US Army MIRADCOM) and Cullis, R. N., (C) "Multi-environment Active RF Seeker (MARFS)(U)," US Army Missile Research and Development Command, November 1, 1976.

3. Lewinski, D. J., Echard, J. D., Rausch, E. O., Piper S. O., and Eaves, J. L., *Stationary Target Detection and Classification Studies, Final Report*, US Army Electronics Research and Development Command, No. DELCS-TR-76-0961-F, April 1979.

4. Stovall, R. E., *A Gaussian Noise Analysis of the "Pseudo-Coherent Discriminant"*, Lincoln Laboratory, Massachusetts Institute of Technology, Technical Note 1978-46, December 29, 1978.

5. Berkowitz, R.S., *Modern Radar Analysis, Evaluation, and System Design*, New York, Wiley, 1965.

6. Skolnik, M. I., *Introduction to Radar Systems*, New York, McGraw-Hill, 1962.

7. Crispen, Jr., J.W. and Siegel, K.M., *Methods of Radar Cross-Section Analysis*, New York, Academic Press, 1968.

DISTRIBUTION

	No. of Copies
Headquarters, Department of the Army Office of the DCS for Research Development and Acquisition ATTN: DAMA-ARZ Room 3A474, The Pentagon Washington, D C 20310	1
Headquarters Department of the Army ATTN: DAMA-WMS	1
LTC Horton	1
Washington, D C 20310	
US Army Research and Standardization Group (Europe) ATTN: DRXSN-E-RX	1
Dr. Alfred K. Nedoluha	1
Box 65 FPO New York 90510	
Commander US Army Foreign Science and Technology Center Federal Office Building 220 7th Street, NE Charlottesville, Virginia 22901	1
Commander US Army Research Office ATTN: Dr. R. Lontz P.O. Box 1211 Research Triangle Park North Carolina 27709	1

DISTRIBUTION (Continued)

	No. of Copies
Commander US Army Training and Doctrine Command Fort Monroe, Virginia 23351	1
Commander US Army Combined Arms Combat Development Activity Fort Leavenworth, Kansas 66027	1
Commander US Army Armor Center Directorate for Armor Aviation ATTN: ATSB-AAD-MS, LTC Don Smart Fort Knox, Kentucky 40121	1
Commander US Army Aviation Center ASH Special Study Group ATTN: ATZQ-ASH-SSG-D	1
COL D. W. RUNDGREN Fort Rucker, Alabama 36362	1
Commander US Army Aviation Center ATTN: AT2Q-D-C	1
M. Jim Burwell Fort Rucker, Alabama 36362	1
Project Manager TADS/PNVS ATTN: DRCPM-AAH-TP	1
COL C. Patnode P.O. Box 209 St. Louis, Missouri 63166	1
Project Manager Smoke and Obscurants Aberdeen, Maryland 21005	1

DISTRIBUTION (Continued)

	No. of Copies
US Army Materiel Development and Readiness Command	
ATTN: Dr. Gordon Bushy	1
Dr. James Bender	1
Dr. Edward Sedlak	1
5001 Eisenhower Avenue Alexandria, Virginia 22333	
Commander US Army Armament Command Rock Island, Illinois 61202	1
Commander US Army Armaments R&D Command Picatinny Arsenal	
ATTN: DRDAR-FCD-W	1
Dover, New Jersey 07801	
Commander US Army Armaments R&D Command Ballistic Research Laboratories	
ATTN: DRDAR-DLB, Mr. R. McGee	1
Aberdeen Proving Ground, Maryland 21005	
Commander US Army Electronics R&D Command	
ATTN: DRSEL-TL-I, Dr. Jacobs	1
DRSEL-CT, Dr. R. Buser	1
Fort Monmouth, New Jersey 07703	
Commander US Army Electronics R&D Command CS & TA Laboratory	
ATTN: DELCS-R, Mr. D. Foiani	1
Fort Monmouth, New Jersey 07703	1
Commander US Army Electronics Command NV & EO Laboratories	
ATTN: DELNV-SI, Mr. W. Ealy	1
Fort Belvoir, Virginia 22060	

DISTRIBUTION (Continued

	No. of Copies
Commander US Army Electronics R&D Command Harry Diamond Laboratories ATTN: DELHD-DBB, Mr. H. Edward	1
Dr. Stan Kuta	1
DELHD-R-RS—C	1
Mr. Greg Cirincione	1
DELHD-R-RSD	1
Mr. Tom Gleason	1
2800 Powder Mill Road Adelphi, Maryland 20783	
Atmospheric Sciences Laboratory US Army Electronics Command ATTN: Dr. Mishri L. Vatsia White Sands Missile Range, New Mexico 88002	1
Director Office of Missile Electronic Warfare ATTN: DELEW-M-ST, Mr. Jim Hardison White Sands Missile Range, New Mexico 88002	1
Commander US Army Aviation R&D Command ATTN: DRDAV-EV, Dr. G. Marner	1
DRDAV-EOP(S), Mr. M. Jackson	1
P.O. Box 209 St. Louis, Missouri 63166	
Commander US Army Aviation Command Foreign Intelligence Office ATTN: Mr. Bert Carney P.O. Box 209 St. Louis, Missouri 63106	1
Commander US Army Mobility Equipment Research and Development Command Fort Belvoir, Virginia 22060	1

DISTRIBUTION (Continued)

	No. of Copies
Director US Army Air Mobility Research and Development Laboratory Ames Research Center Moffett Field, California 94035	1
Commander US Army Tank Automotive Development Command ATTN: DRDTA-RWL Warren, Michigan 48090	1
Director Naval Research Laboratory ATTN: Code 5300, Radar Division, Dr. Skolnik	1
Code 5370, Radar Geophysics Br	1
Code 5460, Electromagnetic Prop Br Washington, DC 20390	1
Office of Naval Research/Code 221 ATTN: D. C. Lewis 800 N. Quincy Street Arlington, Virginia 22217	1
Chief of Naval Research Department of the Navy Washington, DC 20390	1
Commander Naval Air Development Center Sensors and Avionics Technology Directorate Radar Division/Tactical Radar Branch ATTN: Code 3024, Mr. M. Bowdren Warminster, Pennsylvania 18974	1
Commander US Naval Weapons Center ATTN: Mr. Robert Moore China Lake, California 93555	1
Commander Code 3173 Naval Weapons Center ATTN: Dr. Alexis Shlanta China Lake, California 93555	1

DISTRIBUTION (Continued)

	No. of Copies
Commander Center for Naval Analyses ATTN: Document Control 1401 Wilson Boulevard Arlington, Virginia 22209	1
Commander US Naval Surface Weapons Center Dahlgran, Virginia 22448	1
Commander US Naval Electronics Lab Center San Diego, California 92152	
Pacific Missile Test Center Code 3253 ATTN: Charles Phillips Point Mugu, California 93042	1
Naval Surface Weapons Center ATTN: Mary Tobin WR42 White Oak, Maryland 20910	1
Commander AFGL ATTN: RADC/ETEN, Dr. E. Alshuler Hanscom Air Force Base Massachusetts 01731	1
Commander Rome Air Development Center ATTN: R. McMillan, OCSA James Wasielewski, IRRC Griffiss Air Force Base, New York 13440	1 1
Commander US Air Force, AFOSR/NP ATTN: LT COL Gordon Wepfer Bolling Air Force Base Washington, DC 20332	1

DISTRIBUTION (Continued)

	No. of Copies
Commander	
US Air Force Avionics Laboratory	
ATTN: D. Rees	1
CPT James D. Pryce, AFAL/WE	1
Dr. B. L. Sowers, AFAL/RWI	1
Wright Patterson Air Force Base, Ohio 45433	
Commander	
AFATL/LMT	
ATTN: Charles Warren	1
D. Dingus	1
C. Brown	1
Commander	
US Air Force Armament Laboratory	
Eglin Air Force Base, Florida 32542	
Commander	
Defense Documentation Center	
ATTN: DDC—TCA	1
Cameron Station	
Alexandria, Virginia 22314	
Director of Defense Research and Engineering	
ATTN: Mr. Leonard R. Weisberg	1
Dr. G. Gamota	1
Room 3D1079, The Pentagon	
Washington, DC 20301	
Director	
Defense Advanced Research Projects Agency	
1400 Wilson Boulevard	
Arlington, Virginia 22209	1
IIT Research Institute	
ATTN: GACIAC	1
10 West 35th Street	
Chicago, Illinois 60616	
Executive Chairman JTCG-MD/WP-2	
ATTN: ADTC/SD 3, Mr. John Johnson	1
Air Force Armaments Laboratory	
Eglin Air Force Base, Florida 32542	

DISTRIBUTION (Continued)

	No. of Copies
Science and Technology Division Institute of Defense Analysis ATTN: Dr. Vincent J. Corcoran 400 Army-Navy Drive Arlington, Virginia 22202	1
Environmental Research Institute of Michigan Radar and Optics Division ATTN: Dr. A. Kozma Dr. C. C. Aleksoff P. O. Box 618 Ann Arbor, Michigan 41807	1 1
Georgia Institute of Technology Engineering Experiment Station ATTN: James Gallager 347 Ferst Drive Atlanta, Georgia 30332	1
Dr. P. E. Tannenwald Division 8 MIT Lincoln Laboratory Lexington, Massachusetts 02173	1
Dr. H. R. Fetterman Division 8 MIT Lincoln Laboratory Lexington, Massachusetts 02173	1
Dr. D. R. Cohn MIT National Magnet Lab Albany Street Cambridge, Massachusetts 02132	1
Environmental Research Institute of Michigan Infrared and Optics Division ATTN: Anthony J. LaRocca Robert L. Spellicy P.O. Box 618 Ann Arbor, Michigan 48107	1 1

DISTRIBUTION (Continued)

	No. of Copies
Director Calspan Corporation ATTN: R. Kell P.O. Box 235 Buffalo, New York 14221	1
US Army Materiel Systems Analysis Activity ATTN: DRXSY-MP Aberdeen Proving Ground, Maryland 21005	
Dr. J. G. Castle Physics Department University of Alabama 4701 University Drive, NW Huntsville, Alabama 35807	1
Director Ballistic Missile Defense Advanced Technology Center ATTN: ATC-D	1
ATC-O	1
ATC-R	1
ATC-T P.O. Box 1500 Huntsville, Alabama 35807	1
DRCPM-HF, Colonel Robert J. Feist	1
DRCPM-RK	1
DRSMI-YL	1
DRSMI-Z (F10)	1
DRSMI-T, Dr. Kobler	1
Mr. Dobbins	1
-T, Mr. W. Leonard	1
-TE, Mr. Lindberg	1
Mr. Todd	1
Mr. Pittman	1
-TEM, Mr. Harraway	1
-TEO, Mr. Ducote	1

DISTRIBUTION (Concluded)

	No. of Copies
DRSMI-TEO, Mr. Sitton	1
-TER, Mr. Low	1
-TES, Mr. French	1
-TEG, Mr. Cash	1
-TEL, Mr. Mangus	1
Mr. Green	1
Dr. Emmons	1
Dr. Alexander	25
Mr. Barley	1
Mr. Grass	1
Mr. Rast	1
Mr. Mullins	1
-C, Mr. K. Evans	1
Mr. T. Dilworth	1
Mr. H. Burnam	1
Mr. D. Peterson	1
Mr. W. Griffith	1
Mr. J. Baumann	1
-TR, Dr. Hartman	1
Dr. Guenther	1
Dr. Gamble	1
-TBD	3
-TI (Reference Set)	1
(Reference Copy)	1
DRSMI-LP, Mr. Voigt	1
-E, Director	1
-TRADOC LNO	1

-8